

Anisotropic Phase Transitions of Hard-Spheres Confined in Hard Walls

Byoung Jip Yoon

Department of Chemistry, Kangnung National University, Kangnung, Kangwondo 210-702, Korea

Received May 29, 2001

Monte Carlo simulations of hard-spheres confined in parallel hard walls have been carried out extensively at various densities and for various wall distances. The compressibility factors in the directions parallel and normal to the wall have been calculated from the radial free space distribution function (RFSDF) with the results showing that the compressibility factors normal to the wall are smaller than those in parallel direction and that a solid phase is formed in the direction normal to the wall while a fluid phase remains in the parallel direction. An order parameter is found to classify the phases whether a system (or a molecule) is in a fluid or a solid state. The compressibility factors of narrow wall are very small compared to those when the wall is put away. A plausible mechanism of the rise of sap in xylem vessel has been proposed.

Keywords : Radial free-space distribution function, Hard-wall, Order parameter, Anisotropic phase transition, Sap rise.

Introduction

The hard-sphere system is a simple model but it often represents dense fluid and solid systems reasonably. The systems of hard-spheres in a wall or near a wall have been examined by molecular dynamics^{1,2} and the Monte Carlo (MC) method³⁻⁵ and they have been also studied theoretically.⁶⁻⁹

Different from the hard-spheres in a bulk phase, the hard-spheres near a wall have reduced-dimensional motion, *i.e.*, the two-dimensional hard-discs near a wall are pushed against the wall and are constrained to a quasi-one-dimensional motion.² It is also found that the hard-spheres in a wall have a directional anisotropy. The pressure parallel to the wall and normal to the wall observed by molecular dynamics simulations are different.¹ The pressure normal to the wall was lower than the parallel one, however their phase difference was not observed. The phase separation in confined system is of interest in general.^{10,11} In this paper, the hard-spheres confined in parallel hard walls at various densities and for various wall distances have been extensively studied by the MC method and the compressibility factors parallel and normal to the wall are calculated using the radial free space distribution functions (RFSDF), differently from the velocity analysis method as in the usual molecular dynamics simulations. The RFSDF is found to be a very useful function to calculate various thermodynamic properties such as the pressure, entropy (or chemical potential)¹²⁻¹⁵ and even the compressibility.¹⁶ It is not easy to differentiate the parallel and normal pressure to the wall of the hard-sphere system by an MC method, since the velocity components of molecules are not calculated with MC method and the pressure components are not given analytically for this hard-sphere system. However, the RFSDFs parallel and normal to the wall are defined, and the two different compressibility factors parallel and normal to the

wall are calculated from the slope of each function.

Method

The RFSDF, $\zeta(r)$, is obtained in the MC procedure by the following ratio:

$$\zeta(r) = \frac{\text{Acceptances of displacement of } r}{\text{Trials of displacement of } r} \quad (1)$$

where r is the distance reduced with hard-sphere diameter σ . The RFSDF represents the cavity structure formed by neighboring molecules. When the cavity is not isotropic, we can define the function in a directional way. The (radial) free space distribution function parallel to the wall, $\zeta_{\parallel}(r)$, is defined and calculated by attempting the trials of move only to the parallel direction to the wall, and that normal to the wall, $\zeta_{\perp}(r)$, is calculated by the same way but the trials of move are performed only to the normal direction to the wall. The RFSDF starts from 1 at $r = 0$ and decreases exponentially, in general. Therefore it has been expressed well in the following form¹⁷

$$\zeta_{\parallel}(r) = \exp(-a_{\parallel}r - b_{\parallel}r^2) \quad (2)$$

and

$$\zeta_{\perp}(r) = \exp(-a_{\perp}r - b_{\perp}r^2). \quad (3)$$

With the same way to the exact relation between the compressibility factor and RFSDF^{17,19} in the case of usual symmetric boundary condition (see for an example Eq. (3.9) of ref. 18), the compressibility factor parallel to the wall, $p_{\parallel}V/RT$, and that normal to the wall, $p_{\perp}V/RT$, are calculated, respectively, by the slope of the logarithm of each RFSDF at $r = 0$, as follows.

$$\frac{p_{\parallel}V}{RT} = 1 + \frac{2}{3} a_{\parallel} \quad (4)$$

$$\frac{p_{\perp}V}{RT} = 1 + \frac{2}{3} a_{\perp} \quad (5)$$

The MC simulations are carried out at various densities and for various wall distances. The periodic boundary condition is applied only to the Y-Z plane and the walls are put perpendicular to the X-axis departed from the distance L . The number density, $\rho = N/V$, used in this calculation is defined by assuming the volume, V , only where the centers of molecules locate, i.e., the forbidden marginal space of half diameter of hard-sphere molecule from both walls is diminished. And N is the number of molecules used in the simulation. Since the sides of periodic unit box decrease significantly, in Y-Z plane in the case of long wall distance, a large number of molecules must be required in the simulations. Therefore, 500 molecules are used when $L \leq 11\sigma$, 900 molecules are used when $11\sigma < L \leq 31\sigma$, and 1200 molecules when L is longer than 31σ . The initial configuration is a randomly packed one in a unit box and 2 million configurations from the beginning are discarded, and thereafter 3 million samplings are averaged. Among these 3 million samplings, one third of them are for parallel moves only, another one third are for normal moves only, and the other one third are moved to uniform radial directions.

Results and Discussion

Testing the validity of this method of anisotropic calculations in Eqs. (4) and (5), the compressibility factors, $p_{\parallel}V/RT$ and $p_{\perp}V/RT$ are obtained to be 7.00 and 6.45 (at $\rho\sigma^3 = 0.8839$, $L/\sigma = 6$) and 2.71 and 2.66 (at $\rho\sigma^3 = 0.4714$, $L/\sigma = 7$), respectively. These values are in good agreement with the molecular dynamics calculations of Alley and Alder,¹ that are 7.03, 6.31, 2.71, and 2.57, respectively. The RFSDFs are plotted in Figure 1, in which $\zeta_{\parallel}(r)$ has the deeper slope at $r = 0$ but larger value at long distance than $\zeta_{\perp}(r)$ does. The compressibility factors and the coefficients for the least square fit values of RFSDF to Eqs. (2) and (3) were listed in Table 1 for several wall distances along various densities and

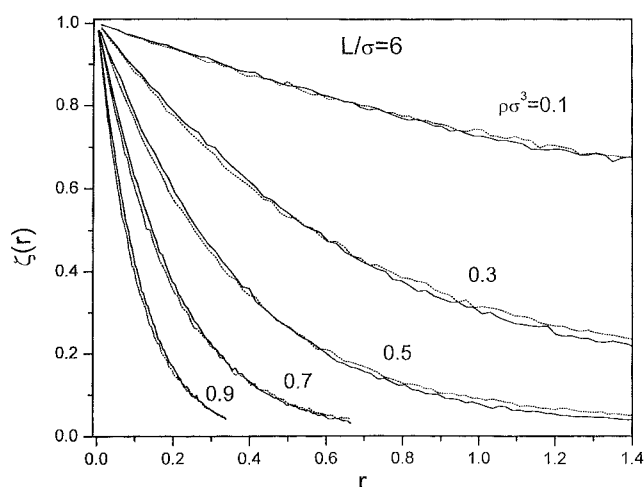


Figure 1. The directional RFSDFs of $L/\sigma = 6$. The solid lines are $\zeta_{\perp}(r)$ and dotted lines are $\zeta_{\parallel}(r)$, respectively. The densities $\rho\sigma^3$ are denoted on the curves.

in Table 2 at several densities along various wall distances. In general, the compressibility factors parallel to the wall are larger than the respective ones normal to the wall. And both compressibility factors are smaller than those when the wall is put away. The compressibility factors of short wall distances ($L/\sigma \leq 6$) are much smaller than those when the wall disappears. The molecules near the wall are two-dimensionally packed against the wall and thus they have large free spaces. $n(\sigma/2)$ is the contact value of the wall and hard-sphere molecules for the density profile along X-axis. At very low densities the wall repels the molecules, and therefore the highest peak is off the surface of the wall. At

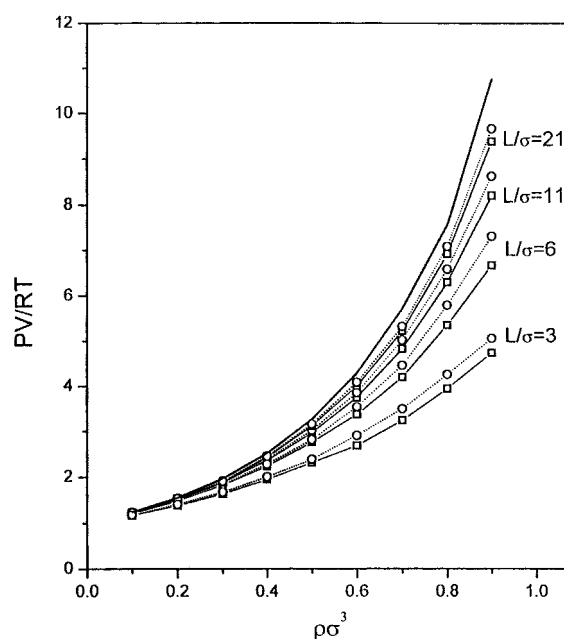
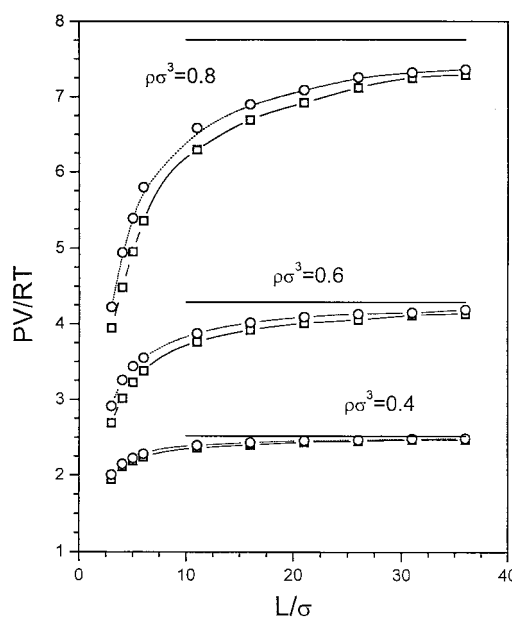
Table 1. The compressibility factors and the coefficients for RFSDF at various densities

$\rho\sigma^3$	$n(\sigma/2)$	$p_{\parallel}V/RT$	$p_{\perp}V/RT$	a_{\parallel}	b_{\parallel}	a_{\perp}	b_{\perp}
$L/\sigma = 3$							
0.1	0.87	1.18	1.17	0.2757	-0.02056	0.2527	-0.02710
0.2	1.05	1.41	1.38	0.6130	-0.05305	0.5724	-0.05734
0.3	1.19	1.67	1.63	1.008	-0.09200	0.9469	-0.08358
0.4	1.40	2.00	1.95	1.503	-0.1527	1.418	-0.1137
0.5	1.72	2.39	2.32	2.084	-0.2167	1.973	-0.1360
0.6	1.87	2.91	2.68	2.862	-0.3487	2.525	0.3164
0.7	2.23	3.50	3.24	3.748	-0.5460	3.358	0.4652
0.8	2.88	4.26	3.93	4.885	-1.101	4.401	1.284
0.9	3.34	5.56	4.73	6.082	-1.222	5.598	5.021
$L/\sigma = 6$							
0.1	0.72	1.23	1.22	0.3442	-0.03190	0.3262	-0.01729
0.2	0.94	1.51	1.49	0.7647	-0.07523	0.7281	-0.04123
0.3	1.22	1.85	1.82	1.270	-0.1269	1.230	-0.07254
0.4	1.52	2.28	2.24	1.918	-0.2107	1.853	-0.09146
0.5	1.85	2.82	2.76	2.725	-0.3099	2.632	-0.06884
0.6	2.37	3.54	3.37	3.816	-0.5271	3.556	0.4546
0.7	3.00	4.46	4.20	5.192	-0.6926	4.796	1.576
0.8	4.12	5.79	5.35	7.188	-2.358	6.521	2.622
0.9	4.94	7.31	6.67	9.460	-1.357	8.498	10.003
$L/\sigma = 11$							
0.1	0.69	1.23	1.23	0.3509	-0.03005	0.3407	-0.02298
0.2	0.89	1.53	1.51	0.8000	-0.07799	0.7684	-0.05241
0.3	1.25	1.91	1.89	1.362	-0.1361	1.331	-0.1003
0.4	1.62	2.39	2.36	2.089	-0.2234	2.039	-0.1237
0.5	2.10	3.03	2.98	3.049	-0.3602	2.967	-0.1377
0.6	2.69	3.87	3.76	4.304	-0.5630	4.138	0.06814
0.7	3.52	5.02	4.82	6.016	-0.9219	5.731	0.8711
0.8	4.56	6.58	6.29	8.371	-1.989	7.938	2.548
0.9	6.09	8.67	8.19	11.50	-1.590	10.78	6.340
$L/\sigma = 21$							
0.1	0.63	1.24	1.23	0.3581	-0.03251	0.3505	-0.02627
0.2	0.88	1.54	1.53	0.8109	-0.07387	0.8011	-0.06290
0.3	1.22	1.91	1.89	1.365	-0.1363	1.335	-0.1014
0.4	1.60	2.46	2.44	2.182	-0.2253	2.154	-0.1631
0.5	2.11	3.16	3.12	3.241	-0.3949	3.178	-0.2352
0.6	2.86	4.09	4.00	4.628	-0.6682	4.505	0.03102
0.7	3.87	5.32	5.22	6.479	-0.6423	6.328	0.1075
0.8	5.23	7.08	6.92	9.123	-0.7533	8.873	2.270
0.9	7.09	9.67	9.39	13.00	-3.918	12.58	4.126

Table 2. The compressibility factors and the coefficients for RFS-DF of various wall distances

L/σ	$n(\sigma/2)$	p_{\parallel}/RT	p_{\perp}/RT	a_{\parallel}	b_{\parallel}	a_{\perp}	b_{\perp}
$\rho\sigma^3 = 0.4$							
3	1.40	2.00	1.95	1.503	-0.1527	1.418	-0.1137
4	1.44	2.15	2.11	1.717	-0.1797	1.664	-0.08857
5	1.48	2.22	2.18	1.833	-0.1196	1.777	-0.07080
6	1.47	2.28	2.24	1.918	-0.2107	1.853	-0.09146
11	1.52	2.39	2.36	2.089	-0.2204	2.039	-0.1237
16	1.51	2.42	2.40	2.148	-0.2228	2.099	-0.1286
21	1.60	2.46	2.44	2.182	-0.2253	2.154	-0.1631
26	1.68	2.47	2.45	2.200	-0.2262	2.176	-0.1662
31	1.77	2.48	2.47	2.222	-0.2333	2.199	-0.2043
36	1.82	2.49	2.47	2.232	-0.2356	2.206	-0.2033
$\rho\sigma^3 = 0.6$							
3	1.87	2.91	2.68	2.862	-0.3487	2.525	0.3164
4	2.08	3.25	3.01	3.374	-0.5858	3.015	0.5281
5	2.26	3.43	3.22	3.648	-0.5788	3.330	0.5610
6	2.35	3.54	3.37	3.816	-0.5271	3.556	0.4546
11	2.69	3.87	3.76	4.304	-0.5630	4.138	0.06814
16	2.87	4.01	3.91	4.515	-0.5297	4.371	0.1232
21	2.86	4.09	4.00	4.628	-0.6682	4.505	0.03102
26	2.83	4.13	4.05	4.691	-0.6268	4.575	-0.02613
31	2.95	4.14	4.11	4.716	-0.5419	4.664	-0.2864
36	2.95	4.19	4.13	4.779	-0.6594	4.696	-0.2286
$\rho\sigma^3 = 0.8$							
3	2.88	4.22	3.94	4.828	-0.8548	4.413	0.7432
4	3.22	4.94	4.48	5.908	-1.438	5.223	3.101
5	3.60	5.38	4.95	6.574	-1.393	5.922	4.200
6	3.84	5.79	5.35	7.188	-2.358	6.521	2.622
11	4.56	6.58	6.29	8.371	-1.989	7.938	2.548
16	5.10	6.89	6.69	8.840	-1.199	8.534	2.783
21	5.23	7.08	6.92	8.873	-0.910	8.823	1.920
26	5.25	7.25	7.11	9.374	-2.053	9.171	1.099
31	5.41	7.32	7.21	9.487	-1.759	9.317	0.7622
36	5.15	7.36	7.29	9.537	-0.4351	9.430	0.7724
41	5.03	7.42	7.33	9.635	-0.6790	9.499	0.5478

high densities, the molecules are pushed against the wall, and the highest peak is at the surface. These data in Table 1 and 2 are plotted in Figures 2 and 3, respectively. There exist fluid-to-solid phase transitions in the normal direction to the wall around $\rho\sigma^3 = 0.5-0.6$. This is not clear in the scale as in Figure 2, however the difference between the compressibility factors in parallel and normal direction plotted in Figure 4 shows the phase difference obviously. Whenever the fluid-to-solid phase transitions occur, the coefficient b has been changed from minus to plus,¹⁴⁻¹⁷ and this is not the exception in this case. In Table 1, the sign of coefficient b is switched from minus to plus between $\rho\sigma^3 = 0.5$ and 0.6. Therefore the coefficient b must be an order parameter to classify the phases whether the system is a fluid phase (when b is negative) or a solid phase (when b is positive). As is well known,²⁰ the negative logarithms of the distribution functions are the corresponding potentials of average force (in units of kT), and their gradients yield the average forces in the given

**Figure 2.** The compressibility factors of various L denoted on the curves. The circles connected with dotted lines are for the parallel values, and the squares with solid lines are for the normal values. The uppermost thick solid line is for the compressibility factor of no walls [ref. 17].**Figure 3.** The same as Figure 2, however the compressibility factors are plotted along wall distance. The uppermost thick lines of each density are of no walls [ref. 17].

set of particles.¹⁸ When b is negative (fluid phase), the mean field force at large distance is smaller than that of equilibrium position (at $r = 0$). This means that once the thermal pressure (bigger than the force at $r = 0$) is given onto the molecule by a kinetic collision, the molecule can slide out from the equilibrium position. On the contrary, when b is positive (solid phase), since the force at large distance is

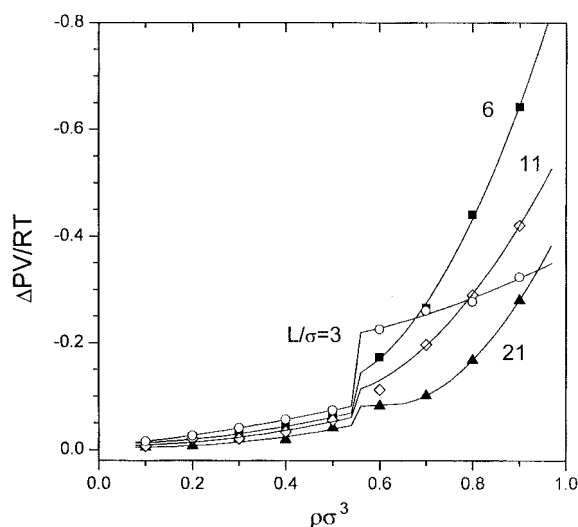


Figure 4. The differences of compressibility factors normal to the wall from those parallel to the wall of several wall distances listed on the curves. The lines are least square fits and each break point was chosen approximately.

bigger than that at $r = 0$. the molecule is repelled back to the position and is confined in the cell. The fluid-to-solid phase transition occurs around $\rho\sigma^3 \approx 1.0$ for the usual hard-sphere system when the three dimensional periodic boundary condition is applied or the wall-effect disappears.^{21,22} In Figure 4, the transition behavior in case of $L/\sigma = 3$ (The centers of molecules are located within the wall distance of 2σ only.) is a bit different from others, probably because most of molecules are located near the surfaces of wall when the wall is very narrow, and the transition is made at a time, while the transitions are done layer by layer from the surface of wall with the increase of density when the wall distances are long. The phase change regions are not dependent of the wall distance in this hard-sphere system, while in the Lennard-Jones system, a slight change in pore width causes a large change in the freezing/melting hysteresis behavior.²³ With the increase of wall distance, the differences between the compressibility factors in parallel and normal direction become small and the transitions are not clearly seen. The RFSDFs, $\zeta_1(r)$ and $\zeta_-(r)$, are calculated in a space-averaged way. However, it is of interest to calculate $\zeta_1(r)$ and $\zeta_-(r)$ along X-axis and to see the phase changes depending on the distance from the wall, since the pressure along X-axis is proportional to the density profile² and the behaviors of molecules near the wall are different from those more distant from the wall.¹⁴ The compressibility factors depending on the distance from the wall are calculated from RFSDF by spacing the positions of molecules in the X-axis finely and are plotted in Figure 5 that shows a very similar behavior to Figure 10 of ref. 2. The molecules near walls show the more anisotropic behavior than the molecules more distant from the surface. According to the sign of the coefficient b , the solid phases appear in a patched form at the distances of the multiple of σ from the surface of wall. A close look at the walks in Figure 4 of ref. 4 informs that the molecules at the

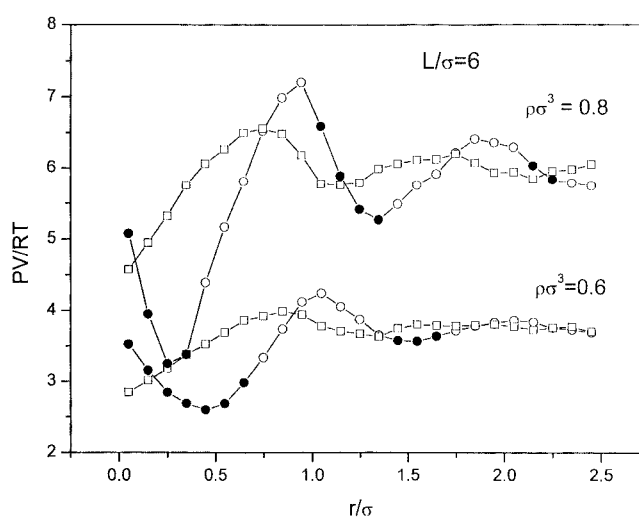


Figure 5. The compressibility factors along X-axis. Squares are the compressibility factors in the parallel direction, and circles are those in the normal direction. Solid circles represent the solid phase while open symbols do the fluid phase.

surface move only in the parallel direction, while the molecules far from the wall move all around, *i.e.*, the molecules at the surface are in the solid state in the normal direction. If a fluid phase is differentiated from the solid phase by the coefficient b , it is of convenience to use this method for studying transition phenomena in various fields such as the melting at a surface.²⁴ Though this simulation is for the hard-sphere interaction with no attractive force, the phenomena of anisotropic phases (a solid phase in the direction normal to the wall and a fluid phase in parallel direction) is associated with the situation of the rise of sap in a xylem vessel, as a climber goes up (a fluid phase) between a narrow crevice by bearing his weight with stretched arms and legs (a solid phase) normal to the wall.

References

- Alley, W. E.; Alder, B. J. *J. Chem. Phys.* **1977**, *66*, 2631.
- Macpherson, A. K.; Carignan, Y. P.; Vladimiroff, T. *J. Chem. Phys.* **1987**, *86*, 4228.
- Liu, K. S.; Kalos, M. H.; Chester, G. V. *Phys. Rev. A* **1974**, *10*, 303.
- Snook, I. K.; Henderson, D. *J. Chem. Phys.* **1978**, *68*, 2134.
- McElroy, J. M. D.; Suh, S.-H. *Mol. Phys.* **1987**, *60*, 475.
- Waisman, E.; Henderson, D.; Lebowitz, L. J. *Mol. Phys.* **1976**, *32*, 1373.
- Giaquinta, P. V.; Parrinello, M. *J. Chem. Phys.* **1983**, *78*, 1946.
- McQuarrie, D. A.; Rowlinson, J. S. *Mol. Phys.* **1987**, *60*, 977.
- Groot, R. D.; Faver, N. M.; van der Eerden, J. P. *Mol. Phys.* **1987**, *62*, 861.
- Christenson, H. K. *J. Phys.: Condens. Matt.* **2001**, *13*, R95.
- Gelb, L. D.; Gubbins, K. E.; Radhakrishnan, R.; Sliwinski-Bartkowiak, M. *Rep. Prog. Phys.* **1999**, *62*, 1573.

12. Yoon, B. J.; Scheraga, H. A. *J. Mol. Struct. (Theochem)* **1989**, *199*, 33.
 13. Yoon, B. J.; Hong, S. D.; Jhon, M. S.; Scheraga, H. A. *Chem. Phys. Lett.* **1991**, *181*, 73.
 14. Yoon, B. J.; Baeck, K. K.; Jeon, S. I. *Chem. Phys. Lett.* **1999**, *301*, 481.
 15. Yoon, B. J. *Bull. Korean Chem. Soc.* **1999**, *20*, 1209.
 16. Yoon, B. J.; Ohr, Y. G. *J. Chem. Phys.* **2000**, *113*, 8149.
 17. Yoon, B. J. *Chem. Phys. Lett.* **1995**, *234*, 35.
 18. Meeron, E.; Siegert, A. J. F. *J. Chem. Phys.* **1968**, *48*, 3139.
 19. Boublik, T. *Mol. Phys.* **1986**, *59*, 775.
 20. Hill, T. L. *Statistical Mechanics*; McGraw-Hill: New York, 1956; Chap. 6.
 21. Barker, J. A.; Henderson, D. *Rev. Mod. Phys.* **1976**, *48*, 587.
 22. Yoon, B. J.; Jhon, M. S.; Scheraga, H. A. *J. Chem. Phys.* **1992**, *96*, 7005.
 23. Radhakrishnan, R.; Gubbins, K. E. *Mol. Phys.* **1999**, *96*, 1249.
 24. Zangwill, A. *Physics at Surfaces*; Cambridge Univ. Press: New York, 1996; Chap. 5.
-